Journal of Ocean, Mechanical and Aerospace
-Science and Engineering-, Vol.5

March 20, 2014

Numerical Visualization of Rudder Inflow as Effect of Increasing Angle of Attack

Najmi. S.M.[a] , Priyanto. A.[a,*], Yasser. M.[a] and Maimun. A[a]

[1]*Marine Technology Centre, Universiti Teknologi Malaysia, 81310 UTM Skudai, Johor, Malaysia*

*Corresponding author: agoes@utm.my

Paper History

Received: 8-January-2014
Received in revised form: 1-March -2014
Accepted: 5-March-2014

ABSTRACT

Thispaper presents a study to examine the characteristics of the rudder inflow (propeller slipstream) using FLUENT v.6 visualization technique. The rotating propeller of 5 blades and semi-spade rudder were set in a uniform flow condition. The rudder distorts the angle-of-attack (AoA) or incident angle to the leading edge of the rudder blade. Time-averaged pressure and velocity field are proposed to analyze the AoA and show similar AoA values of 0°–7° at the region on rudder. However, it increases to 20° by those effects as the inflow comes to the rudder. From the AoA analysis the similar flow pattern is found to be about 7° in terms of the rudder angle. Cautious access is additionally necessary to introduce a reasonable safety against those inflow phenomena that would significantly influence the durability of the rudder.

KEY WORDS: *Rudder Inflow; Angle of Attack; Propeller Slipstream; FLUENT; Velocity Field.*

1.0 INTRODUCTION

Systematic prediction of propulsion system design is crucial towards efficient propulsion. Mainly contributed by the propeller, it is thrusting forward by screw movement and flow passing these twisted edges surrounding it. The hydrodynamic analysis of rotating propeller in vicinity of a rudder is somewhat a complex one. It has become one of the most challenging problems in computational fluid dynamics (CFD) validation [1], [2] and it has been investigated conventionally using potential theory for decades. As the year progressing, CFD has now become a practical tool in solving propeller flow problems via Reynolds Averaged Navier Stokes (RANS) solver. As ships are becoming larger and their power consumption is also increasing, high axial momentum behind a ship propeller may induce strong cavitation on the surface or discontinuities in the ship rudder. The propeller wake intrinsically has the contracted slipstream tube in the condition of uniform flow. However, it has specific angles of attack to the left (port) and right (starboard) sides of the rudder blade, which is located behind a propeller as validated by Kim, et.al [2] as shown in Fig.1.

Figure 1.a): Flow paint streaks on the port side of rudder [2]

Figure 1.b): Flow paint streaks on the starboard side of rudder [2]

The differences in incident flows toward the rudder have affected its lift forces and ships' manoeuvrability. To obtain sufficient lift forces in the rudder, an excessive rudder angle may be required in the actual operation of ship. On the other hand, an increased rudder angle induces a large amount of violent rudder cavitation, and may cause cavitation erosion of its surface. Securing sufficient lift has often conflicted with the trials of reducing rudder cavitation in both full-spade and semi-spade rudders. Rudder cavitation could have a negative effect on ships from hydrodynamic and structural viewpoints. If strong cavitation on the rudder results in serious damage, considerable time and cost would be necessary to maintain or repair a rudder eroded by cavitation. Therefore, it is very important to inspect flow behaviour around the rudder when the propeller is ahead of the

rudder.

2.0 PROPELLER AND RUDDER

A five bladed B-series typed B 5-88 propeller is considered. The propeller is intended to propel the LNG carrier. It is a fixed pitch and the axis of the propeller is parallel with the free stream direction. The extistance of hull as shown in Fig.2 was used to simulate the non-uniform incoming wake pattern. In the simulation, the non-uniform wake pattern was defined to replace the available default function in the Ansys FLUENT. The placement of hull before propeller and rudder hence should make an adequate simulation results due to the defined non-uniform wake source.

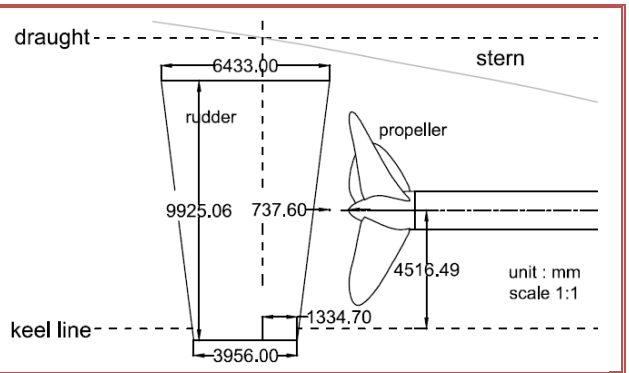

Figure 2: Sketch of semi-spade rudder incident flow caused by propeller wake

3.0 MODELING SET UP

As dealing with complex geometry like propeller and rudder, it is quite difficult for direct simulation of turbulence. Using time averaged technique such as Reynolds Averaged Navier Stokes (RANS), it is used to simplify the instantaneous RANS [3]. The equations are as following:

$$\rho \frac{\partial u_i}{\partial x_i} = 0 \tag{1}$$

$$\rho \frac{\partial}{\partial x_j}(u_i u_j) = -\frac{\partial p}{\partial x_i} + \rho \frac{\partial}{\partial x_j}\left[v\left(\frac{\partial u_i}{\partial x_j} + \frac{\partial u_j}{\partial x_i}\right)\right] - \frac{\partial}{\partial x_j}\left(-\rho \overline{u_i' u_j'}\right) \tag{2}$$

In which u_i and $u_j(i, j=1, 2, 3)$ are time averaged velocity components; x_i and $x_j(i,j= 1, 2, 3)$ are coordinates in surge, heave, and sway directions respectively; density of fluid (ρ), time averaged pressure (p), kinetic viscosity of water (υ), and Reynolds stress term $\left(-\rho \overline{u_i' u_j'}\right)$. For proceeding calculations, standard k epsilon turbulence model is used. The transport equations of standard k epsilon turbulence model are as follows:

$$\rho \frac{Dk}{Dt} = \frac{\partial}{\partial x_j}\left(\alpha_{k\mu_{eff}} \frac{\partial k}{\partial x_j}\right) + P - \rho\varepsilon \tag{3}$$

$$\rho \frac{D\varepsilon}{Dt} = \frac{\partial}{\partial x_j}\left(\alpha_{k\mu_{eff}} \frac{\partial k}{\partial x_j}\right) + C_{1\varepsilon}\frac{\varepsilon}{k}P - C_{2\varepsilon}\rho\frac{\varepsilon^2}{k} \tag{4}$$

In which k represents the turbulent kinetic energy, ε is dissipation ratio of k, t being time, while ρ and x_j are already defined in equation (1) and (2). μ_{eff} is the turbulent kinetic energy, P represents the production of turbulence kinetic energy. α_k= 1.0 and α_ε = 1.3 are the inverse effective Prandtl number of k and ε respectively, while $C_{1\varepsilon}$ = 1.44 and $C_{2\varepsilon}$= 1.92 act as constants of the model.

Table 1: Geometrical parameters of propeller and rudder

Items	symbol	value
diameter	*D*	7700mm
pitch-diameter ratio	*P/D*	0.94
expanded area ratio	A_E/A_O	0.88
number of blade	*z*	5
rudder height/*D*	*L/D*	1.289
rudder height/chord	482	565

Steady analysis of propeller-rudder interaction was analyzed using multiple reference frame method to simulate the interaction between the rotor and stator domains. The mesh elements consist of two parts; moving mesh and stationary mesh. Unstructured grids are used in both domains. The size of computational domain was referred to [4] for the open water test (OWT 1). A description to Fig. 3 is available in Table.2, where *Lmr* is measured from middle hub, *D* and *L* are referring to propeller diameter and domain length.

Table 2: Open Water Tests (OWT) computational domain

Items	OWT1 w/o rudder	OWT2 with rudder
Ds	3.6D	3.6D
Dr	1.4D	1.4D
Lsi	2D	2D
Lso	6D	6D
Lr	1.4D	0.75D
Lmr	0.7D	0.214D

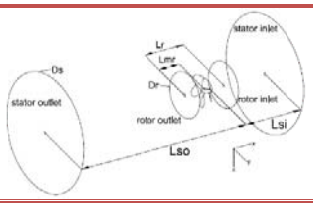

Figure 3.a): Computational configuration domain

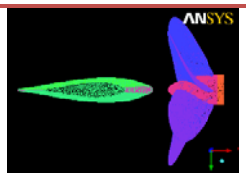

Figure 3.b): Definition of Angle of Attack AoA (α) ahead of rudder leading edge

The flow regions are assigned into several categories:

- The inlet – velocity inlet assumed, assigned value, the characteristic dimension and turbulence model values
- The outlet – pressure outlet is assumed
- Propeller blades and shaft – non viscous wall

- Outer boundary – non viscous wall.

Tests were performed at full scale. The rudder rests at three designated positions; AoA= 0^0,-7^0 and -20^0 positioned 0.0958D from top of hub as per classification requirement. Information regarding angle of attack is available in Fig. 3b). The solver setting was based on [1]. The advance speed, V_A was fixed at 6.687 m/s. The stator inlet was designated as velocity inlet, while the stator outlet was designated as pressure outlet with normal atmospheric pressure.

Regarding the solver setting, pressure based calculation with absolute velocity formulation and steady flow were selected. Total number of mesh elements for rudder AoA = 0^0,-7^0 and -20^0 are averaged at 1.8millions while OWT 1 and OWT 2 counts for 1.485 millions in average. Fluid domain was specified as fresh water and aluminium for solid domain.

Proceeding to solution methods, simple pressure-velocity coupling was selected with second order upwind for momentum turbulent kinetic energy and turbulent dissipation rate. Detailing the boundary conditions, velocity inlet was selected for stator inlet with intensity and viscosity ratio of 10 for the turbulent specification method. Pressure outlet is defined for the stator outlet with zero gauge pressure and similar turbulent specification as stator inlet. All convergence rests at 0.001.

4.0 RESULTS AND DISCUSSION

Figures 4 – 9 show that the pressure distribution at starboard side was higher than the one at port side, it means that the flow goes on the negative AoA. Time-averaged pressure field are proposed to analyze the AoA and show similar AoA values of 0°,–7° at the region on rudder. However, it increases to -20° by those effects as the inflow comes to the rudder. The maximum pressures are located at absolute Z = 0.7R near the upper rudder face view from port side and lower rudder face of starboard side. These may happen due to clockwise movement of the propeller slipstream. This is the phenomenon where tip vortices sourcing from propeller attacks rudder surface.

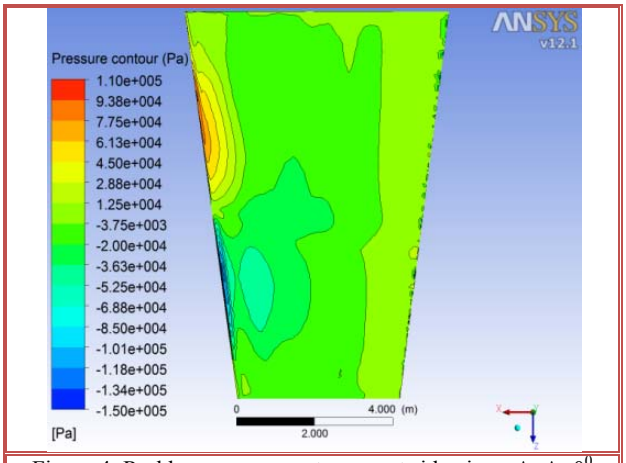

Figure 4: Rudder pressure contours port side views AoA=0^0

As the rudder deflects more, significant pressure drop can be noticed at absolute Z = 0.7R port side of rudder leading edge. This is likely the occurrence of cavitation inception, in which the lower pressure values as indicated in the Figures 5 and 6 have crucial effects on the cavitation and flow separation, as claimed by [4,5].

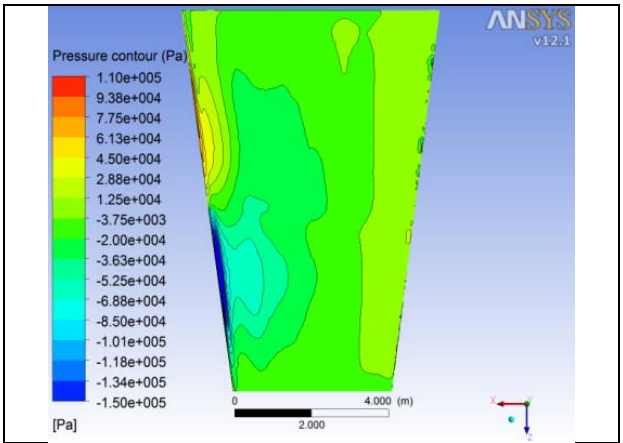

Figure 5: Rudder pressure contours port side views AoA=-7^0

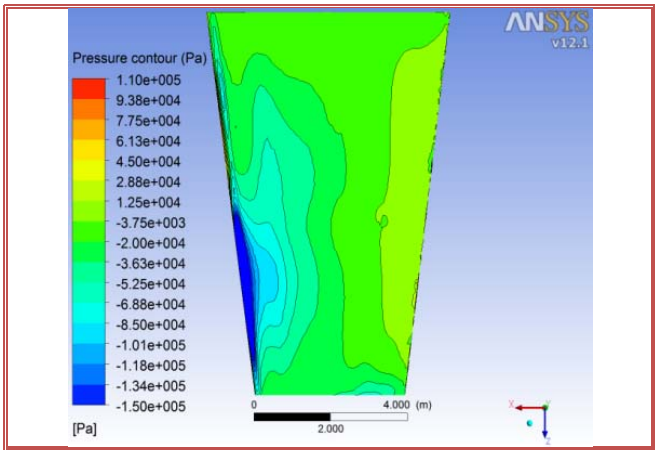

Figure 6: Rudder pressure contours port side views AoA=-20^0

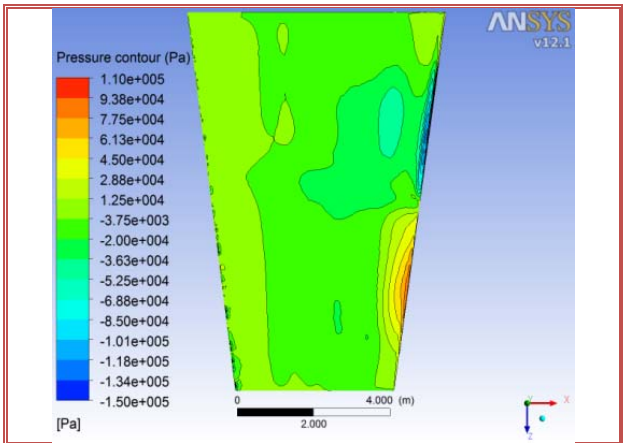

Figure 7: Rudder pressure contours starboard side views AoA=0^0

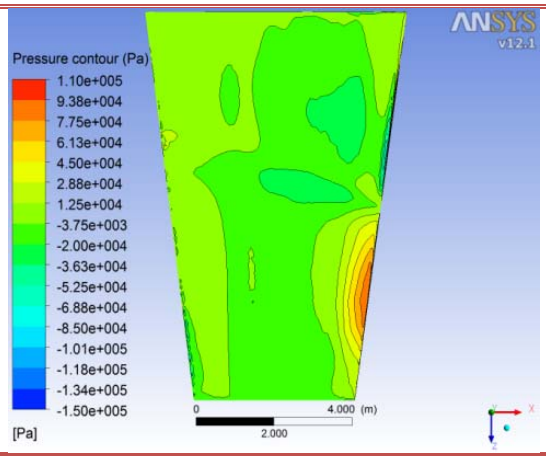

Figure 8: Rudder pressure contours port side views AoA=-7^0

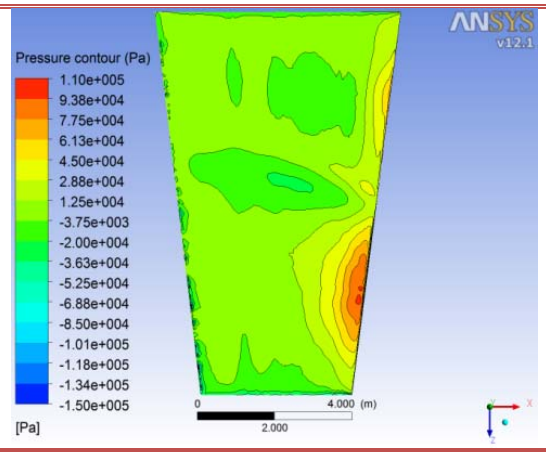

Figure 9: Rudder pressure contours port side views AoA=-20^0

Next Figs 10 – 12 represent rudder ambient velocity contours in XZ cross sectional plane positioned right after the rotational domain (X= -0.291m).

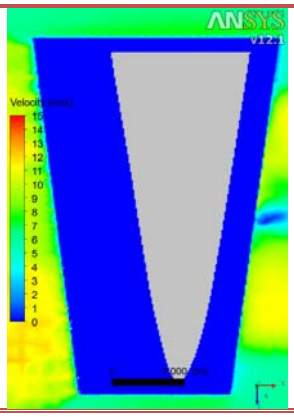

Figure 10: Velocity contours of surrounding fluids starboard side views at rudder angle AoA=0^0

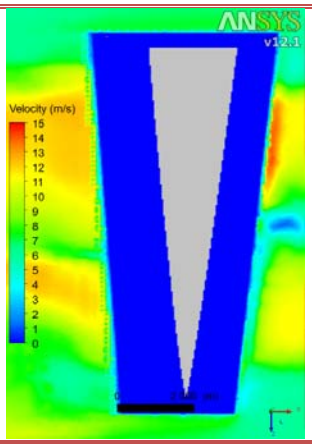

Figure 11: Velocity contours of surrounding fluids starboard side views at rudder angle AoA=-70^0

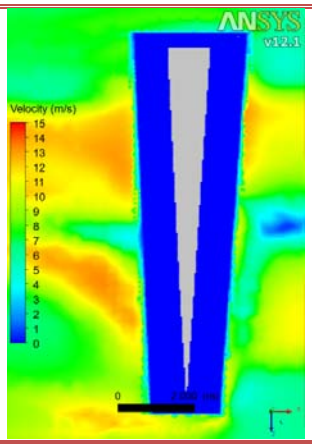

Figure 12: Velocity contours of surrounding fluids starboard side views at rudder angle AoA=-20^0

As we can see, significant amount of velocity difference are noticed at the region of Z = 0.7R, near top side of rotating propeller. The amount of velocity becomes larger as the rudder started to deflect and slightly lower as the rudder deflects to -20^0. An indicator of tip vortex cavitation may prevail here, in which regions of high velocity tailing from propeller tip is a sign of lower pressure compared to fluid at rest (Bernoulli's law).This may happen due to typically low advance velocity on the upper side of a rotating propeller, viewed from propeller back. High propeller blades angle of attack is the cause to the lower pressure and therefore experiences higher velocity.

5.0 CONCLUSION

The flow of propeller-rudder interaction has been investigated using RANS modelling. Significant differences in terms of induced velocity field and pressure distribution could be noticed. Prediction and inspection of flow behaviour could be made possible in order to locate the cavitation susceptibility as early

precaution to structural assessment of rudder. These characteristics are important for further assessment especially durability of propeller and strength assessment for safety manoeuvring. This moving reference frame method provides an adequate solution for the determination of time accurate solution to predict the propeller and rudder interaction.

ACKNOWLEDGEMENTS

All results were obtained from the research project "Modelling propeller and rudder induced forces for deep drafted vessels in Restricted Water". Thanks to Universiti Teknologi Malaysia (UTM) and Ministry of Higher Education (MOHE), Malaysia for the financial support to this project denoted by R.J130000.7824.4F049.

REFERENCE

[1] Mitja Morgut, E. N. (2009), Comparison of Hexa-Structured and Hybrid-Unstructured Meshing Approaches for Numerical Prediction of the Flow Around Marine Propellers, *First International Symposium on Marine Propulsors smp'09, Trondheim, Norway: 7*.

[2] Van, S.H., Kim, W.J., Yoon, H.S., Lee, Y.Y. (2006), *Flow measurement around a model ship with propeller and rudder*, Experiments in Fluids 40, Springer – Verlag: 533-545.

[3] Chun-yu Guo , W.-t. H. a. S. H. (2010), *Using RANS to Simulate the Interaction and overall Performance of Propellers and Rudders with Thrust Fins*, Journal of Marine Science and Application 9: 323-327.

[4] Jan Kulczyk, L. S., Maciej Zawiślak (2007), Analysis Of Screw Propeller 4119 Using The Fluent System, *Archives of Civil And Mechanical Engineering 7(4): 9*.

[5] Yavuz Hakan Ozdemira, S. B., Tamer Yılmaza (2009), Flowfield Analysis Of A Rudder By Using Computational Fluid Dynamics, *International Advanced Technologies Symposium (IATS'09), Karabuk, Turkey 5*.